CORE
Metadata, citation and similar papers at core.ac.uk
Provided by NASA Technical Reports Server

DEPARTMENT OF PHYSICS
SCHOOL OF SCIENCES & HEALTH PROFESSIONS
OLD DOMINION UNIVERSITY
NORFOLK, VIRGINIA

TECHNICAL REPORT PTR-85-2

RADIATION EFFECTS INDUCED IN PIN PHOTODIODES BY 40- AND 85-MeV PROTONS

By

J. Becher, Principal Investigator

R. L. Kernell, Co-Principal Investigator

C. S. Reft

Progress Report
For the period ending January 31, 1985

Prepared for the
National Aeronautics and Space Administration
Goddard Space Flight Center
Greenbelt, Maryland 20771

Under
Research Grant NSG-5289
Walter J. Fowler, Technical Monitor
Laboratory for Astronomy & Solar Physics

Submitted by the
Old Dominion University Research Foundation
P. O. Box 6369
Norfolk, Virginia 23508

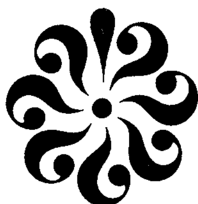

April 1985

RADIATION EFFECTS INDUCED IN PIN PHOTODIODES BY 40- AND 85-MeV PROTONS

By

J. Becher[1], R. L. Kernell[2] and C S. Reft[3]

ABSTRACT

PIN photodiodes were bombarded with 40- and 85-MeV protons to a fluence of 1.5×10^{11} p/cm^2, and the resulting change in spectral response in the near infrared was determined. The photocurrent, dark current and pulse amplitude were measured as a function of proton fluence. Changes in these three measured properties are discussed in terms of changes in the diode's spectral response, minority carrier diffusion length and depletion width. A simple model of induced radiation effects is presented which is in good agreement with the experimental results. The model assumes that incident protons produce charged defects within the depletion region simulating donor type impurities.

[1] Associate Professor, Department of Physics, Old Dominion University, Norfolk, Virginia 23508.

[2] Professor, Department of Physics, Old Dominion University, Norfolk, Virginia 23508.

[3] Research Associate, Department of Radiology, University of Chicago, Illinois 60637.

TABLE OF CONTENTS

	Page
ABSTRACT	iii
INTRODUCTION	1
EXPERIMENTAL PROCEDURE	2
EXPERIMENTAL RESULTS	5
DISCUSSION OF RESULTS	6
General	6
Determination of Depletion Width	7
Determination of Carrier Diffusion Length	8
DEGRADATION MODEL	9
General	9
Depletion Width	10
Spectral Response	11
Increase of Dark Current	13
SUMMARY	15
REFERENCES	16

LIST OF TABLES

Table		Page
1	Slopes determined from Figure 8 for 40-MeV protons and for 85-MeV protons from similar graph	17

LIST OF FIGURES

Figure		Page
1	Schematic diagram of the experimental arrangement for exciting photodiodes utilizing a monochromator	18
2	Schematic diagram of the experimental arrangement for obtaining pulse height spectra	19
3	Measured quantum efficiency for a typical PIN photodiode used in this work	20
4	The ratio of currents in the irradiated diode to the reference	

TABLE OF CONTENTS (continued)

LIST OF FIGURES (continued)

Figure		Page
	diode as a function of the wavelength at various fluences of 40-MeV protons	21
5	Effect of 40-MeV proton irradiation on the current-voltage characteristic of the photodiode dark current...............	22
6	Effect of 40-MeV proton irradiation on the pulse height spectra taken at 10 V bias.................................	23
7	Preirradiation depletion width plotted as a function of the square root of the applied bias voltage....................	24
8	Effect of 40-MeV proton irradiation on the depletion width at several bias voltages....................................	25
9	Degradation in spectral response for a typical PIN photodiode irradiated with 40-MeV protons. Symbols indicate experimental data; curves are theoretical fits based on model proposed in text..	26
10	Degradation as a function of fluence at selected wavelengths. Symbols indicate experimental data; curves are theoretical fits based on model proposed in text.......................	27
11	Effect of 40-MeV proton irradiation on PIN photodiode dark current..	28

INTRODUCTION

Silicon PIN photodiodes are frequently used in satellite astronomy for detecting radiation in the visible and near infrared portions of the electromagnetic spectrum. Although not as sensitive as photomultiplier tubes, these diodes are relatively cheap, low-power, compact devices with a wide spectral response. PIN photodiodes are often used as detectors in an optical data link. It is desirable to know the response of these photodiodes to the space radiation environment Radiation induced effects in PIN photodiodes have been investigated using gammas (Ref 1) and neutrons (Ref 2). Because some orbits, such as those proposed for the NASA Space Telescope, subject the observatory to bombardment by protons, it is of interest to investigate the vulnerability of PIN photodiodes to protons.

It is useful to note that PIN photodiodes are similar to solar cells in that both are p-n junction devices which differ in their mode of operation and junction characteristics. A substantial amount of work exists on the effects of electrons and gamma radiation on silicon solar cells (Refs 3,4,5) with the emphasis being on the reduction of their output power. On the other hand, the work reported here is concerned with irradiation-induced degradation in spectral response of PIN diodes. A basic difference between solar cells and PIN diodes is the magnitude of their depletion widths. In solar cells a typical depletion width is 1 μm whereas in PIN photodiodes the depletion width is much larger, varying from 10 to 200 μm depending upon the resistivity of the intrinsic region and the operating bias voltage. In this respect PIN Photodiodes are similar to surface barrier detectors. Hence, the irradiation-induced damaged models (Ref 6) developed for solar cells are not directly applicable to PIN photodiodes and models for surface barrier detectors have not been adequately evaluated in terms of their suit-

ability for PIN photodiodes. This paper presents results of spectral response degradation in the near infrared produced by 40- and 85-MeV proton bombardment together with a simple model that accounts for the induced changes in the spectral response, increase in dark current, and changes in the pulse amplitude created by charged particles.

EXPERIMENTAL PROCEDURE

The PIN photodiodes studied in this work are state of the art devices consisting of a p-n junction with a doping profile tailored to produce an intrinsic layer, "i region", between a p layer and an n layer. We investigated six PIN-6D (United Detector Technology) diodes. These diodes have a resistivity of 400 Ω-cm, an antireflection coating which maximizes the response at 850 nm and an active area of $0.2\ cm^2$. These devices were fabricated using the planar diffusion of p and n regions into a heavily doped (less than 1 Ω-cm) semiconductor substrate.

The effect of proton bombardment on these photodiodes was studied by examining the changes in spectral response, dark current, and pulse height. The spectral response of the photodiodes was determined prior to and after irradiation by measuring the photocurrent as a function of wavelength from 500 to 1100 nm. Monochromatic light was obtained from a tungsten halogen lamp dispersed by a grating monochromator whose bandwidth was approximately 8 nm at these wavelengths. To minimize the effect of fluctuations in the light source and electronics, the signal from the test diode was always compared at the time of measurement to that from a similar unirradiated reference diode. This was accomplished by coupling a double-beam attachment to the output slits of the monochromator, one channel being dedicated to the test diode and the other channel to a similar unirradiated reference diode. Figure 1 illustrates this experimental arrangement. The movable mirror in

the double-beam attachment reflected the monochromatic light to either the sample or reference diode. The incident wavelength and the photocurrents of the test and reference diodes were fed to a computer. Repeated measurements of a diode's spectral response showed that the ratio of sample to reference photocurrents was reproducible to within 2 percent. Because the time between completion of proton irradiation and the spectral response measurements was typically about ten minutes, this experiment investigated relatively long term effects associated with cumulative dose rather than short term transient characteristics. The effect of irradiation on the spectral response at wavelength λ after bombardment with a proton fluence ϕ is expressed in terms of the degradation parameter $D(\lambda,\phi)$ defined by

$$D(\lambda,\phi) = \frac{I(\lambda,\phi) - I_D}{I(\lambda,o) - I_{D_o}} \qquad (1)$$

where $I(\lambda,o)$ and $I(\lambda,\phi)$ are the photocurrents before and after irradiation and I_{D_o} and I_D are the corresponding dark currents. The photocurrents used in equation (1) are normalized values in that, as discussed above, they represent ratios of test diode to reference diode values. It should be noted that the parameter $D(\lambda,\phi) = 1$ corresponds to zero degradation and that D becomes smaller as the degradation increases.

The current measured in the biasing circuit includes a dark current whose magnitude is related to the bulk properties (resistivity, minority carrier diffusion length, etc.) of the photodiode. Changes in these properties induced by irradiation were monitored by repeated dark current measurement. The dark current of the photodiode was measured with the configura-

tion shown in Figure 1 by blocking the light at the entrance slits of the monochromator. The dark current measurement had an uncertainty of about 3 percent.

Changes in the depletion width of the photodiode were studied by recording the pulse height of the voltage generated by the accumulated charge created by ionizing protons passing through the device. These pulse height spectra were obtained by reducing the fluence rate used in the degradation exposures (typically about 10^9 p/cm^2-sec) to about 1.5 x 10^4 p/cm^2-sec. A schematic of the pulse height arrangement is shown in Figure 2. This detection system was calibrated by injecting a known charge into a calibrated load capacitor, thereby relating the voltage from the multichannel analyzer to the charge created by the ionizing irradiation. We estimate a 5 percent uncertainty in the depletion widths inferred from the pulse height spectra.

The proton irradiations were performed with the isochronous cyclotron at the University in Maryland. Because of the configuration of the cyclotron target facility, it was convenient to mount the photodiodes on a sample ladder in a chamber which was an integral part of the beam transport system. Since the ladder was remotely controlled, the diodes could be moved into or out of the beam without altering the beam characteristics. The proton fluences were measured by a current monitor and the spatial distribution of the beam was estimated using film. At the energies used (40 and 85 MeV), the beam was relatively stable in intensity and beam profile. We estimate that our fluence measurements had an uncertainty of about 15 percent absolute with a somewhat smaller relative uncertainty among the irradiated samples. Successive exposures, sometimes at different fluence rates, were performed to accumulate dose.

EXPERIMENTAL RESULTS

The spectral response of each diode was measured before and after each irradiation. In view of the fact that we express the spectral response in terms of the ratio of the photocurrents of the tested and reference diodes, it is useful to keep the absolute efficiency in mind. Figure 3 shows a typical quantum efficiency measured prior to irradiation. This curve was obtained by using a calibrated United Detector Technology photodiode to determine the photon flux impinging on the diode. An auxiliary check on the efficiency was made using an NBS calibrated tungsten ribbon source. Changes in the quantum efficiency produced by irradiation with 40-MeV protons are shown in Figure 4 in which the degradation $D(\lambda,\phi)$ is plotted against wavelength from 700 to 1050 nm for several fluences. These data were collected at a bias voltage of 5 V. We note that for a given fluence the degradation becomes more pronounced as the wavelength increases and that, as expected, the efficiency decreases with irradiation dose. In a subsequent section we present a model which accounts for the observed dependence of the degradation on wavelength and fluence.

An increase in dark current with fluence was observed for all diodes. Figure 5 shows the measured dark current for a representative diode as a function of bias voltage at various fluences. Prior to irradiation the dark current varies linearly with the bias voltage at a rate of 0.024 μA/V. As the fluence increases the dark current becomes larger but still varies linearly with bias voltage. However, the rate of increase is larger; for example, at 0.4×10^{10} p/cm^2 the slope is 0 64 μA/V. We observed this linear dependence up to $1\ 0 \times 10^{10}$ p/cm^2. At a fluence of 10.0×10^{10}p/cm^2, the dark current had continued to increase but no longer varied linearly with bias voltage. As will be discussed later, we attribute this increase

of dark current with fluence to a decrease in minority carrier length.

The depletion width was determined from pulse height spectra collected while bombarding the photodiode at a sufficiently low proton fluence rate that negligible damage occurred during the measurement. As we will discuss in the next section, the depletion width is proportional to the pulse height. Figure 6 shows the pulse height spectra for a typical diode taken at 10 V bias after various fluences. Note that the number of counts is plotted as a function of the depletion width inferred from the observed pulse height. The observed change in position of the peak with increasing fluence indicates a decrease in depletion width of the diode.

DISCUSSION OF RESULTS

General

The current produced in PIN photodiodes consists of two components: the drift current created within the depletion width and the diffusion current produced by charge created in the bulk substrate diffusing into the reverse biased junction. Under steady state conditions the current is given by the sum of these. Assuming that the current due to thermal generation of charge is negligible, the total current at a constant bias voltage is given by

$$I(\lambda,\phi) = q\Phi \left(1 - \frac{e^{-\alpha W}}{1 + \alpha L}\right) + q\, p_{no} \frac{D_p}{L} \qquad (2)$$

(Ref 7) where q is the electron charge, Φ is the absorbed photon flux rate, α is the wavelength dependent absorption coefficient, W is the depletion width (which, as we have seen, depends on the proton fluence ϕ), L is the minority carrier diffusion length, D_p is the diffusion coeffi-

cient of holes in the n type bulk, and p_{no} is the thermal equilibrium concentration of holes in the n type silicon. Since the second term is independent of the photon flux, it is essentially the dark current I_D of the device. Making this substitution and using equations (1) and (2), we can write the degradation as

$$D(\lambda,\phi) = \left(1 - \frac{e^{-\alpha W}}{1 + \alpha L}\right) \Big/ \left(1 - \frac{e^{-\alpha W_o}}{1 + \alpha L_o}\right) \quad (3)$$

This equation implies that the spectral degradation is associated with changes in the depletion width and/or diffusion length.

Determination of Depletion Width

In a semiconductor detector the energy lost by ionizing radiation results in the creation of electron-hole pairs (EHP's) within the depletion width; these are collected at the junction. Ideally, the number of EHP's collected by the detector is proportional to the energy lost by ionizing radiation in the depletion region. It is true, of course, that a major portion of a PIN diode's width (about 300 μm) consists of bulk material which is penetrated by ionizing radiation creating EHP's in it path. However, since there is no electric field to collect the charges in this region, they diffuse to the electrodes at a slow rate. Thus, we were able to use a fast charge sensitive preamplifier with a rise time of about 10 ns to accumulate charge created in the depletion width only.

The charge pulse created by the ionizing particle is given by

$$Q = \frac{q\Delta E}{\varepsilon} \quad (4)$$

where q is the charge of the electron, ΔE is the energy deposited by a

single ionizing particle in the depletion region, and ε is the average energy (3.62 eV for silicon) required to create an EHP. The energy lost in the depletion region is given by $\Delta E = W\,(dE/dx)$ where dE/dx is the stopping power for protons in silicon at the appropriate energy. Substituting for ΔE in equation (4) and rearranging, we obtain

$$W = \frac{\varepsilon}{q} \frac{Q}{dE/dx} = 2.26 \times 10^{13} \frac{Q}{dE/dx} \tag{5}$$

Thus, the pulse height of the signal produced by a single incident proton provides a direct measurement of the depletion width. The depletion width measured by us before any appreciable radiation dose was accumulated agreed with the results of Dearnaley and Northrop (Ref 8) in that W_o varied as the square root of the applied bias. Our results for a typical diode are shown in Figure 7. We note that W_o increases at the rate of 6.75 μm/V. This linear dependence was found for all six diodes used in our work; the measured values of W_o varied by less than 5 percent among the diodes. We also found that the value of W_o did not depend on whether we used 40- or 85-MeV protons to produce the charge pulse. This is consistent with equation (4) in that the significant parameter is the energy deposited by the incident particle. The measured value of W_o at 5 volts was 27 μm which is about 20 percent higher than the theoretical value predicted for the 400 Ω-cm material (Ref 7).

Determination of Carrier Diffusion Length

We determined L_o by measuring the photon response of the photodiode and fitting the results to equation (2) using the reported absorption coefficients for silicon (Ref 9) and W_o obtained from our pulse height analy-

sis. This gave $L_o = 200\ \mu m$ which is consistent with the diffusion length predicted for 400 Ω-cm n-type silicon (Ref 10).

DEGRADATION MODEL

General

Irradiation of semiconductors with high energy particles displaces atoms and damages the lattice, thereby introducing new energy levels into the band gap. These defects act as recombination centers which decrease the minority carrier lifetime (Ref 11). Since PIN diodes have large depletion widths, irradiation-induced changes in this region have a significant effect on the diode photocurrent. When silicon surface barrier detectors are irradiated with protons, damage produced in the depletion region increases the depletion width capacitance. Since this capacitance is proportional to the dopant density (Ref 7), the observed increase indicates that the created defects had a net positive charge (donor behavior).

We suggest that the created defects can be represented as impurity dopants whose energy level is located within the forbidden band gap. Thus, the effective displacement site density will increase with radiation; we write this as

$$N(\phi) = N_D + \sigma\ \phi \qquad (6)$$

where $N(\phi)$ is the effective displacement site density, N_D is the impurity dopant density, and σ is the cross section (in cm^{-1}) for defect production. For the PIN diodes investigated by us, the donor impurity dopants in the intrinsic region are $N_D = 1.2 \times 10^{13}\ cm^{-3}$ and in the p layer $N_A = 6 \times 10^{15}\ cm^{-3}$. Since $N_A >> N_D$, the one-sided abrupt junction approxima-

tion can be used to determine the depletion width. In this approximation the depletion width is (Ref 7)

$$W = B\,[N(\phi)]^{-\frac{1}{2}} = B\left(N_D + \sigma\,\phi\right)^{-\frac{1}{2}} \tag{7}$$

In this equation, $B = \sqrt{2\varepsilon_s V/q}$, ε_s is the static dielectric constant, and V is the total voltage applied to the junction. Rearranging equation (7) gives

$$\frac{1}{W^2} = \frac{\sigma\,\phi}{N_D\,W^2{}_o} + \frac{1}{W_o{}^2} \tag{8}$$

where $W_o^2 = B^2/N_D$. Equation (8) can be used to deduce values of σ from our experimental data. We will now use this simple model to discuss the observed changes in depletion width, spectral response, and minority diffusion length (as inferred from the dark current).

Depletion Width

Figure 8 shows W^{-2} plotted as a function of fluence for 40-MeV protons at various bias voltages. A similar figure was obtained at 85 MeV. For fluences below about 10 x 10^{10} p/cm^2, the data show a linear dependence in agreement with our model. Using equation (8) in conjunction with the 5 V bias line of Figure 8 we find (using N_D = 1.2 x 10^{13} p/cm^3) σ = 150 cm^{-1} for 40-MeV protons while at 85 MeV σ = 95 cm^{-1}. These values are generally consistent with those reported (Ref 12) by Bilinski, et al. As shown in Figure 8, σ is dependent on the applied voltage. Even though the linear-

ity of W^{-2} with ϕ is maintained at higher bias voltages, σ decreases with increasing voltage for both 40- and 85-MeV protons. For example, for 40-MeV protons the cross section decreases from 150 cm^{-1} at a bias of 5V to 90 cm^{-1} at 40 V. The cross section will be independent of applied voltage if the defects are produced uniformly throughout the depletion region. This suggests that the observed dependence on voltage is associated with a nonuniform creation of defects within the depletion region.

Table I lists the slopes of the straight line portions of Figure 8 for 40-MeV protons together with the slopes of a similar graph for our 85-MeV data. From equation (8) we note that for a given bias voltage the ratio of the cross sections for two bombarding energies is just the ratio of the corresponding slopes. These ratios for 40- and 85-MeV protons are shown in Table I. This ratio is nearly constant and has an average value of 1.6 ± 0.3. The rate at which defects are created is proportional to the absorbed energy which varies as the stopping power. Using stopping powers of 27.4 and 15.4 MeV/cm for 40- and 85-MeV protons, respectively, we obtain a ratio of 1.8. The fact that this is nearly the same as the observed ratio of the corresponding cross sections strengthens our postulate that the defects produced by irradiation are responsible for the changes in depletion width.

Spectral Response

Changes in depletion width and minority carrier diffusion length produce degradation in the spectral response of the diode. In this section we compare the observed degradation with that predicted by our model. For this purpose the experimental spectral response results at selected fluences are shown as data points in Figure 9. Some of these data points are plotted

at selected wavelengths in Figure 10 in order to show explicitly the dependence of the degradation on wavelength. The curves in Figures 9 and 10 are predictions based on our model; these curves were obtained as follows. The degradation can be determined from equation (3) by using W calculated from equation (5) in conjunction with L determined from equation (2) using reported values (Ref 9) of the wavelength dependent absorption coefficient α. This gives the degradation D in terms of λ and W. We then use the results of equation (8) based on our model to express W in terms of the fluence ϕ, thereby obtaining $D(\lambda,\phi)$. When this is done, the curves drawn in Figures 9 and 10 are obtained using $N_D = 1.2 \times 10^{13}$ cm^{-3} (as given in the specifications of the PIN-6D photodiode) and the following experimentally determined parameters:

$$W_o = 27\ \mu m$$

$$L_o = 200\ \mu m$$

$$\sigma = 200\ cm^{-1}$$

With the exception of the data at the low fluence of 0.05×10^{10} p/cm^2, there is excellent agreement up to 9×10^{10} p/cm^2 between the predictions of our model and the experimental results over the entire wavelength range. Note that the model correctly predicts the rapid degradation in response with wavelength as illustrated in Figure 10. The observed degradation in spectral response deviates from our model above 10×10^{10} p/cm^2 which (as shown in Figure 8) is also the fluence level above which the degradation in W no longer follows the behavior predicted by our model. At these higher fluences the one-sided abrupt junction approximation which is incorporated into our model is no longer valid. The density of irradiation-induced defects has become comparable to the initial dopant density with the result that the interactions between defects and impurities is no longer described

by this simple model. At these fluences, the energy levels of the displacement sites dominate over the dopant.

Increase of Dark Current

The dark current increased with fluence for all the diodes studied by us. This can be understood by considering a modified form of the photon independent term of equation (2).

$$I_D = qn_i^2 \frac{D_p}{N_D L} (e^{qV/kT} - 1) \quad (9)$$

where the relation $p_{no} = n_i^2/N_D$ is used, n_i is the intrinsic carrier concentration, V is the applied voltage, k is Boltzman's constant, and T is the temperature. The factor in parenthesis is included to give the dependence of dark current on voltage. This is the Shockley equation for an ideal diode (Ref 7) with the approximation that $p_{no} >> n_{po}$ used for these diodes because $N_A >> N_D$. We note that the dark current is inversely proportional to L which decreases with fluence resulting in an increase in dark current. This is illustrated in Figure 5 where the dark current is shown as a function of bias voltage at various fluences.

We will discuss the changes in dark current with fluence in terms of the dark current ratio $I_D(\phi)/I_D(0)$. Assuming that D_p and N_D do not change during irradiation (i.e., $\sigma \phi << N_D$), equation (9) leads to

$$\frac{I_D(\phi)}{I_{D_o}(0)} = \frac{L_o}{L} \quad (10)$$

As mentioned previously, the induced defects act as recombination centers which decrease the minority carrier lifetime. This is equivalent to a decrease in the minority carrier diffusion length and can be expressed as (Ref 13)

$$\frac{1}{L^2} = \frac{1}{L_o^2} + K\,\phi \tag{11}$$

where K is the associated degradation parameter. Using equation (10), we get

$$\frac{I_D(\phi)}{I_D(0)} = (1 + K\,L_o^{\;2}\,\phi)^{\frac{1}{2}} \tag{12}$$

This predicted dependence is compared to our experimental results in Figure 11 which shows the square of the dark current ratio versus fluence for 40-MeV protons. Using L_o = 200 μm, the slope of the line gives K = 3.5 x 10^{-6} cm^{-2} compared to a reported value of 6.5 x 10^{-6} cm^{-2} (Ref 12). Thus, for fluences below 10 x 10^{10} p/cm^2, the increase in dark current can be attributed to a decrease in minority carrier diffusion length.

For fluences greater than 10 x 10^{10} p/cm^2, we must consider changes in N_D. In the previous section we argued that the defects ($\sigma\phi$) produced by irradiation become comparable to N_D at the higher fluences. From equation (6), we infer that N_D in equation (8) should be replaced by $N_D + \sigma\,\phi$. This would produce a slight departure from linearity of the square of the dark current ratio versus ϕ at these higher fluences.

SUMMARY

We have investigated the effects of 40- and 85-MeV protons on PIN photodiodes by measuring changes in the photoconductive diode current, dark current and pulse height spectra. We associated the changes in these three measured properties with changes in the diode's spectral response, minority carrier diffusion length, and depletion width. We developed a model which is in good agreement with our experimental results for fluences up to 10 x 10^{10} p/cm^2. The model assumes that the incident protons produce charged defects within the depletion region simulating donor type impurities. From the model we can estimate the useful lifetime of the photodiode as a detector.

It is also possible to use the degradation in spectral response of these diodes to measure the absorbed energy. Rösch et al. (Ref 13) have shown that the neutron-induced change in the optical response of n+p junction silicon diodes can be used to measure the absorbed energy from 0.3 to 14.0 MeV neutrons.

At higher fluences, $\sigma \phi >> N_D$, the model breaks down. The density of irradiation-induced defects becomes comparable to the initial dopant density, and the interactions between defects and impurities is much more complicated than in our simple model. A more rigorous treatment would take into account the location of the irradiation-induced defects within the forbidden band gap and also the thermal stability of these defects.

The work reported here was supported by NASA Grant NSG-5289.

REFERENCES

1. K. W. Mitchell, "Optimizing Photodetectors for Radiation Environments," IEEE Trans. Nucl. Sci. NS-24, 2294-2297 (Dec 1977).

2. A. H. Kalma and W. H. Hardwick, "Radiation Testing of PIN Photodiodes," IEEE Trans. Nucl. Sci. NS-25, 1483-1488 (Dec. 1978).

3. F. Larin, "Radiation Effects in Semiconductor Devices," John Wiley and Sons, New York (1968).

4. H. J. Hovel, "Semiconductors and Semimetals, Vol. 2: Solar Cells," Academic Press (1975).

5. W. E. Horne and M. C. Wilkinson, "Improved Model for Predicting Space Performance of Solar Cells," IEEE Trans. Nucl. Sci. NS-21, 130-137 (Dec. 1974).

6. J. F. Weller and R. L. Statler, "Low Energy Proton Damage to Solar Cells," IEEE Trans. Nucl. Sci. NS-10, 66-70 (Nov. 1963).

7. S. M. Sze, "Physics of Semiconductor Devices," John Wiley and Sons, New York (1969).

8. G. Dearnaley and D. C. Northrop, "Semiconductor Counters for Nuclear Radiations," Spon, 2nd ed. (1966).

9. W. C. Dash and R. Newman, "Intrinsic Optical Absorption in Single-Crystal Germanium and Silicon at 77°K and 300°K," Phys. Rev. 99, 1151-1155 (1955).

10. W. Rosenzweig, H. K. Gummel and F. M. Smits, "Solar Cell Degradation under 1-MeV Electron Bombardment," Bell Syst. Tech. J. 42, 399-414 (1963).

11. J. J. Loferski and P. Rappaport, "Radiation Damage in Ge and Si Detected by Carrier Lifetime Changes: Damage Thresholds," Phys. Rev. 111, 432-439 (1958).

12. J. R. Bilinski, E. H. Brooks, V. Cocca and R. J. Maier, "Proton-Neutron Damage Equivalence in Si and Ge Semiconductors," IEEE Trans. Nucl. Sci. NS-10, 71-86 (Nov. 1963).

13. E. Rösch, G. Weickelt and D. Broström, "Si Photodiodes as Dosimeters for Fast Neutrons," Nucl. Instr. Meth. 10, 47-49 (1972).

TABLE I

Slopes determined from Figure 8 for 40-MeV protons and for 85-MeV protons from similar graph.

Bias (Volts)	40 MeV Slope (x 10^{-5})	85 MeV Slope (x 10^{-5})	Slope Ratio
5	0.171 ± .025	0.107 ± .025	1.6 ± .3
10	0.083 ± .020	0.055 ± .010	1.5 ± .3
20	0.054 ± .005	0.034 ± .005	1.7 ± .3
40	0.025 ± .001	0.015 ± .001	1.7 ± .2

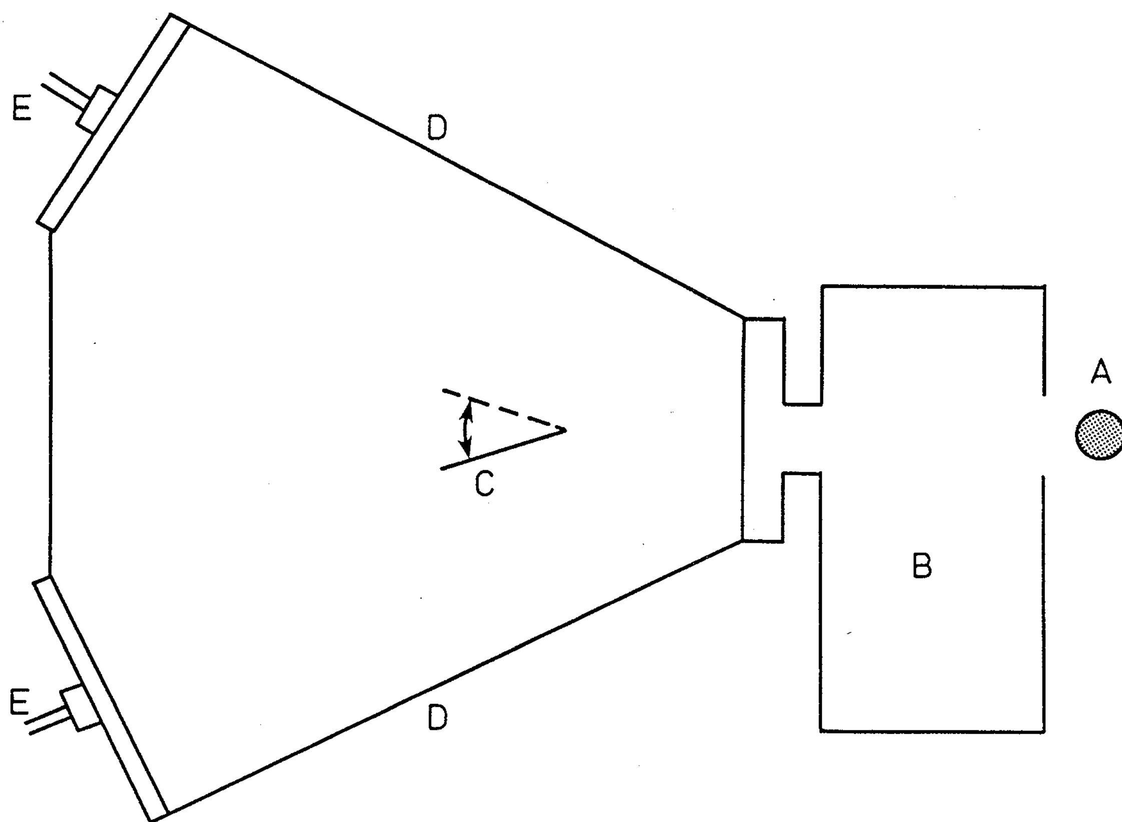

A TUNGSTEN HALOGEN LAMP
B GRATING MONOCHROMATOR
C MOVABLE MIRROR
D DOUBLE BEAM ATTACHMENT
E REFERENCE AND TEST PHOTODIODES

Figure 1. Schematic diagram of the experimental arrangement for exciting photodiodes utilizing a monochromator.

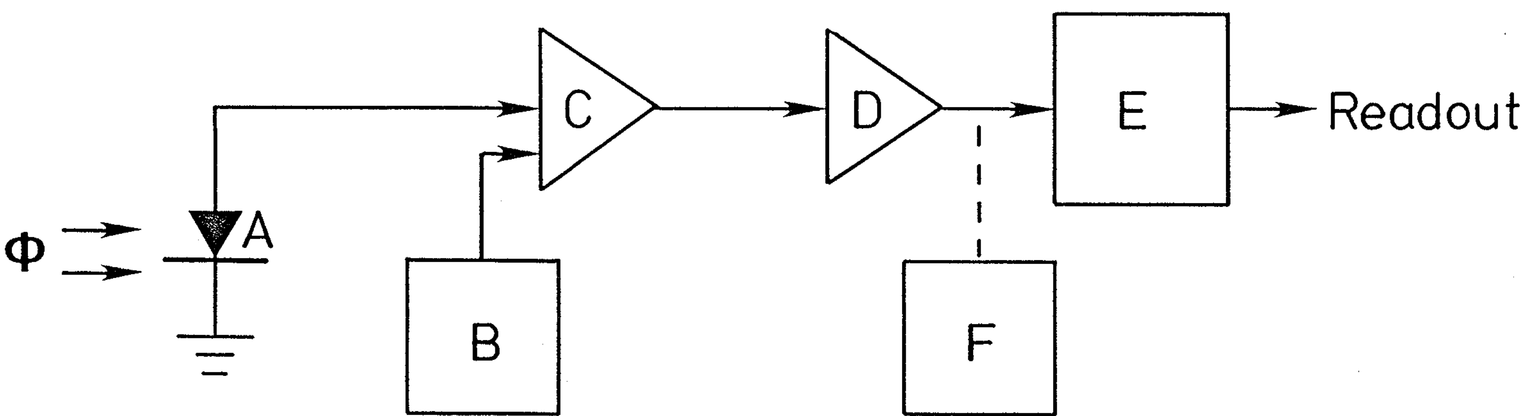

Figure 2. Schematic diagram of the experimental arrangement for obtaining pulse height spectra.

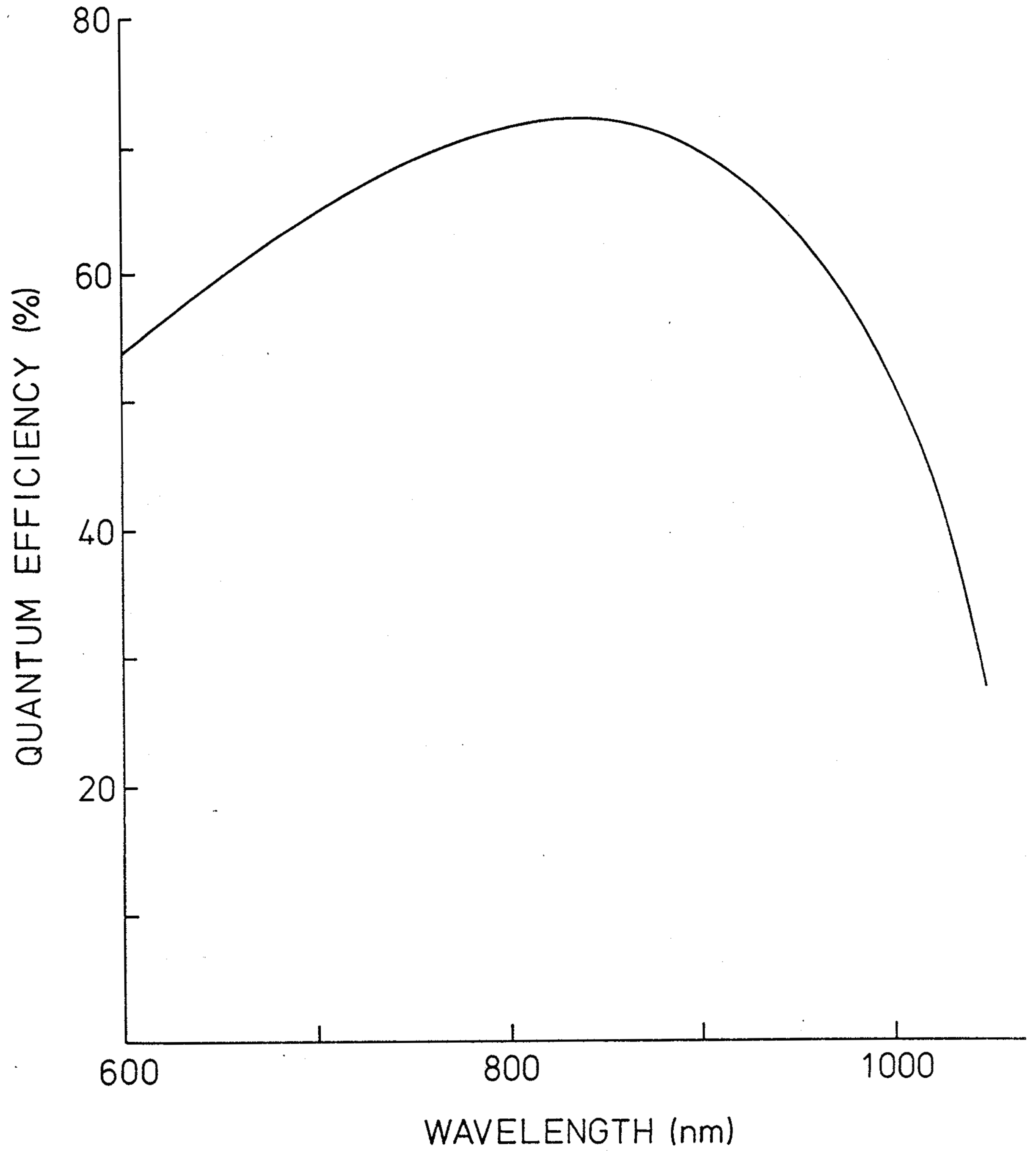

Figure 3. Measured quantum efficiency for a typical PIN photodiode used in this work.

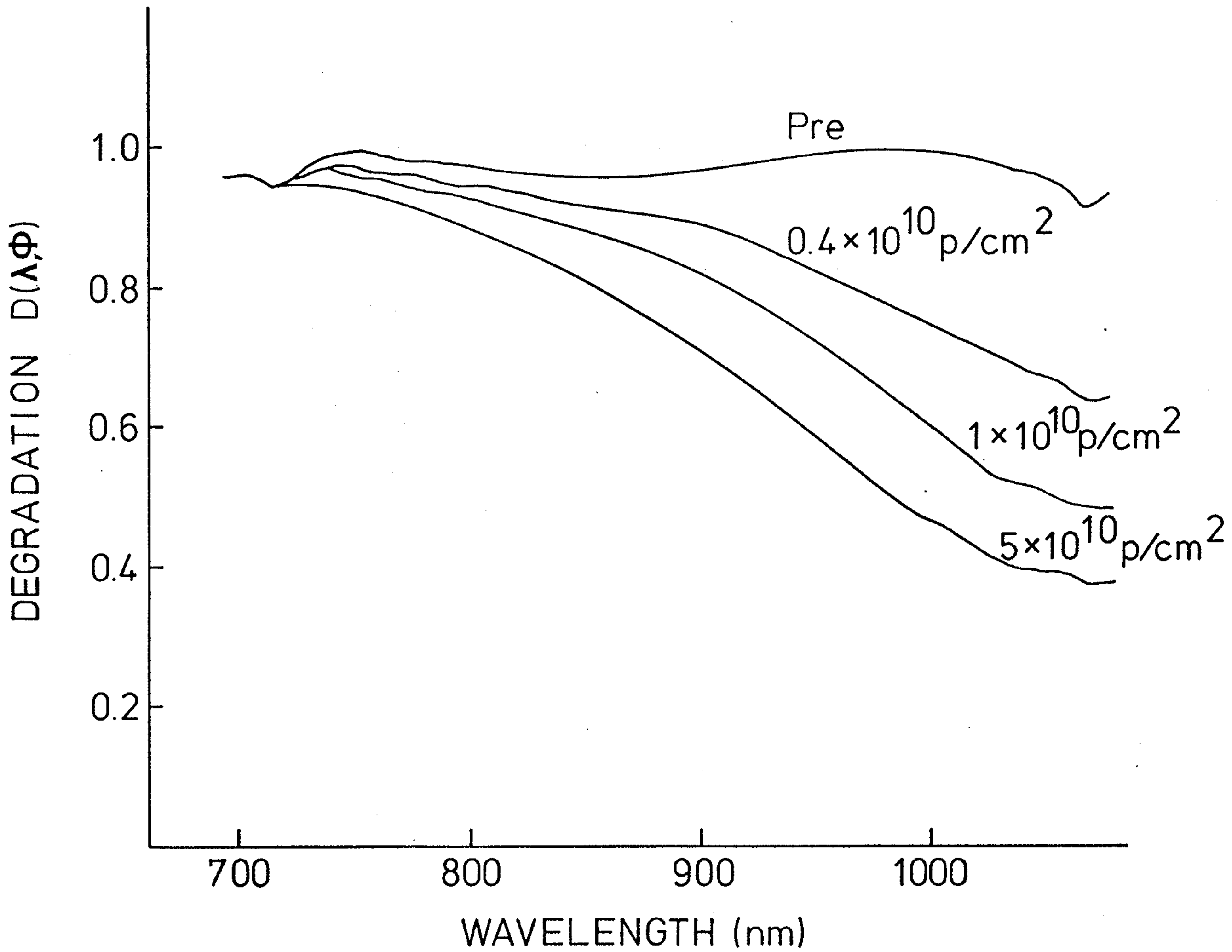

Figure 4. The ratio of currents in the irradiated diode to the reference diode as a function of the wavelength at various fluences of 40-MeV protons.

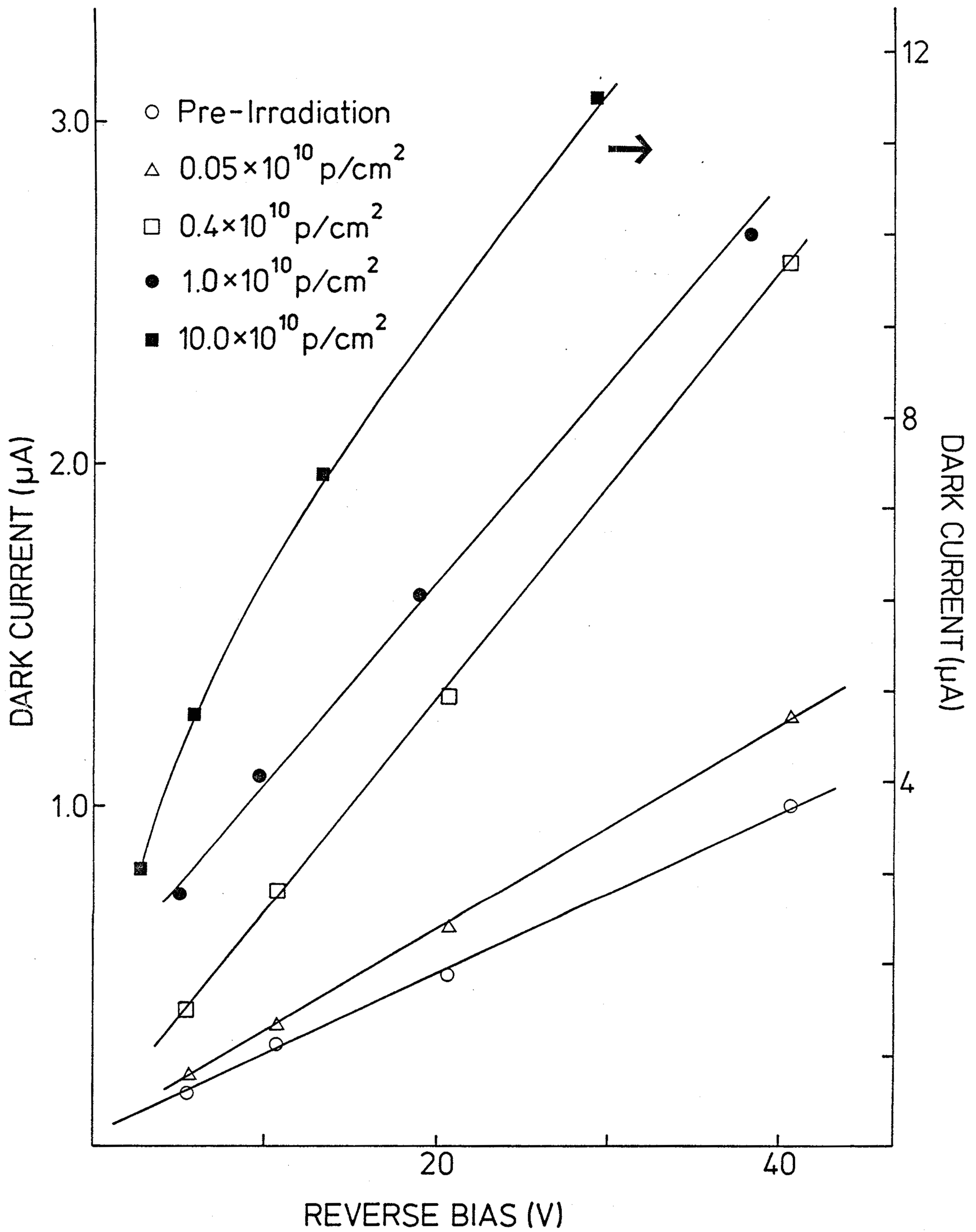

Figure 5. Effect of 40-MeV proton irradiation on the current-voltage characteristic of the photodiode dark current.

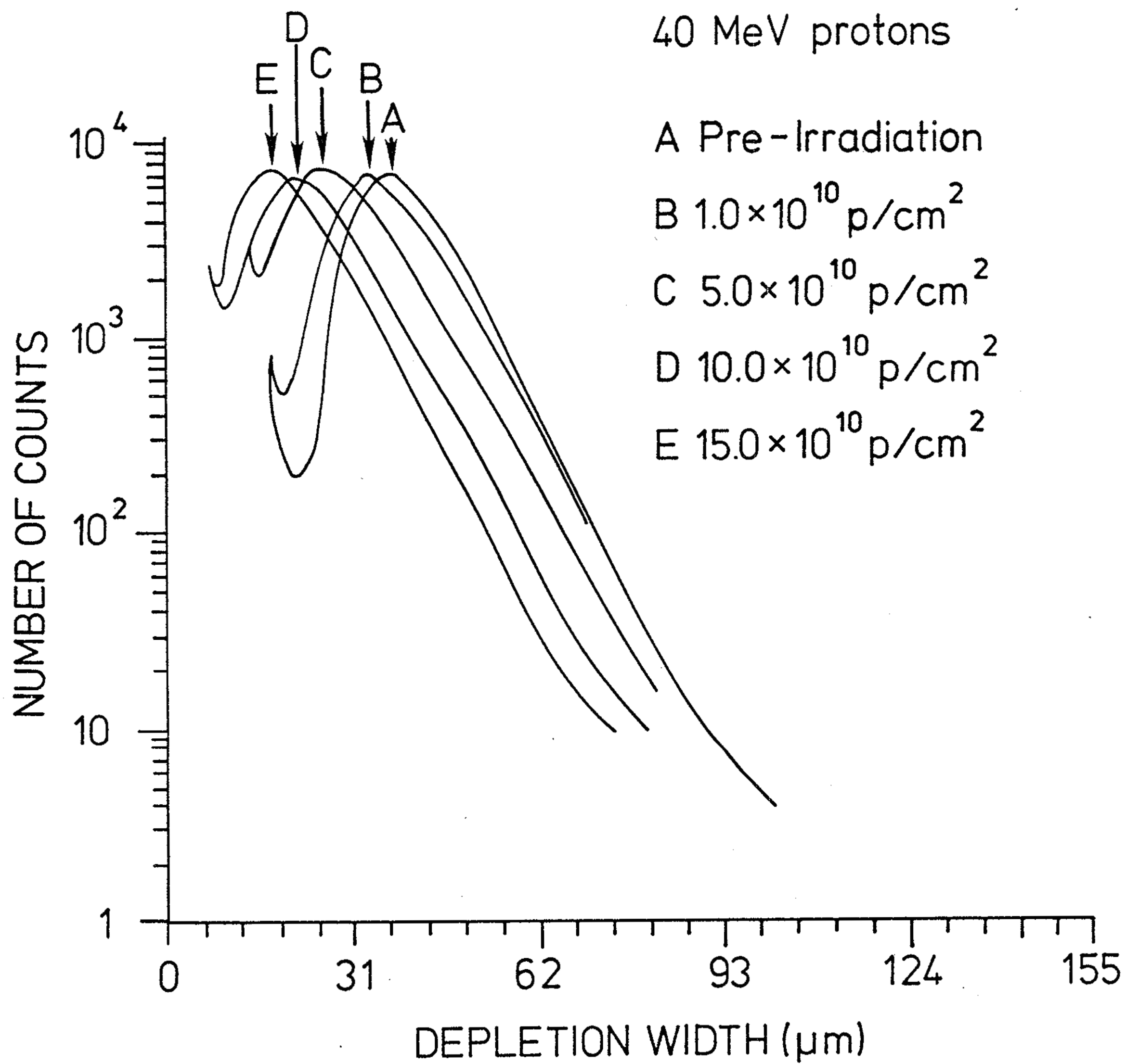

Figure 6. Effect of 40-MeV proton irradiation on the pulse height spectra taken at 10 V bias.

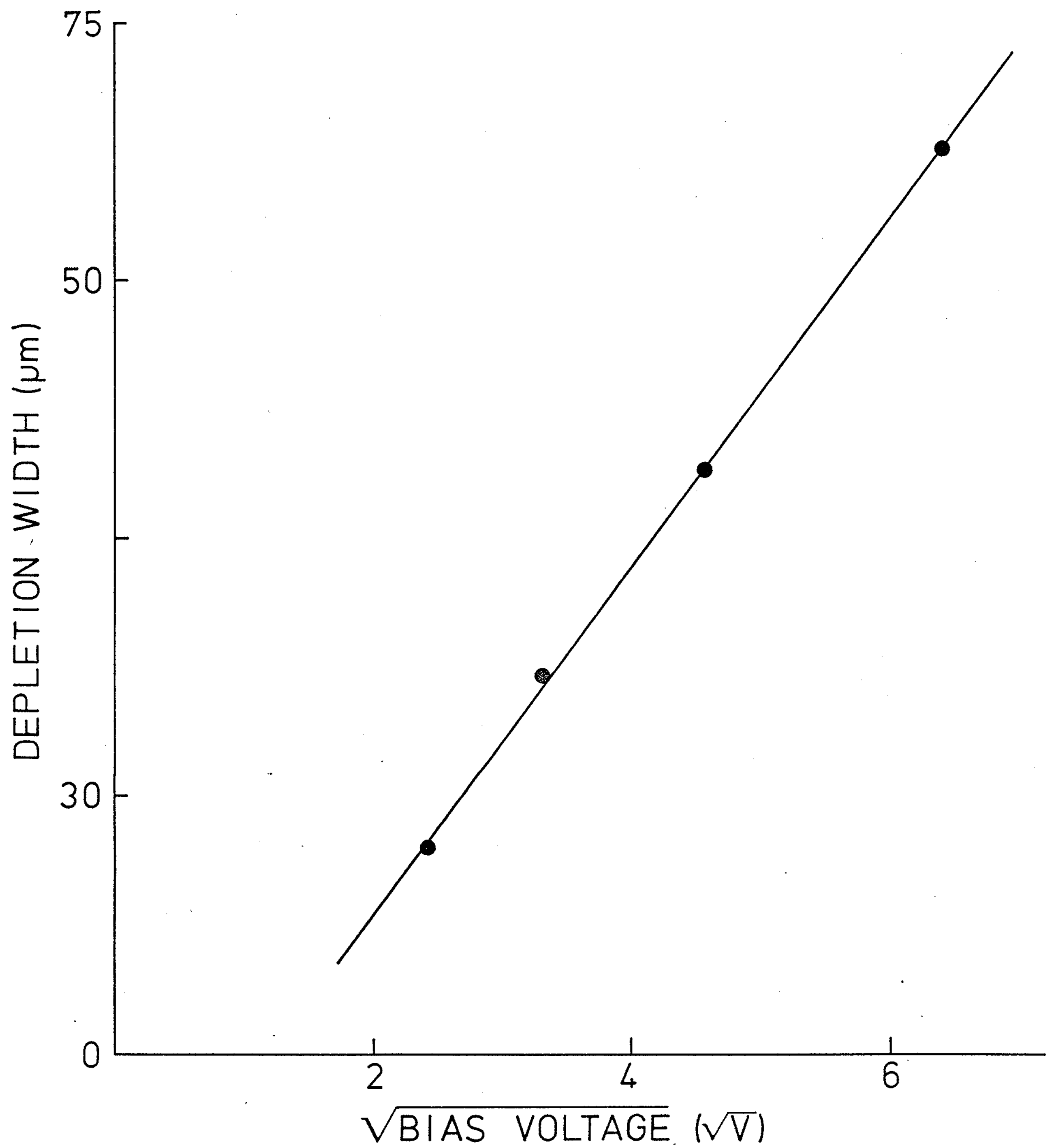

Figure 7. Preirradiation depletion width plotted as a function of the square root of the applied bias voltage.

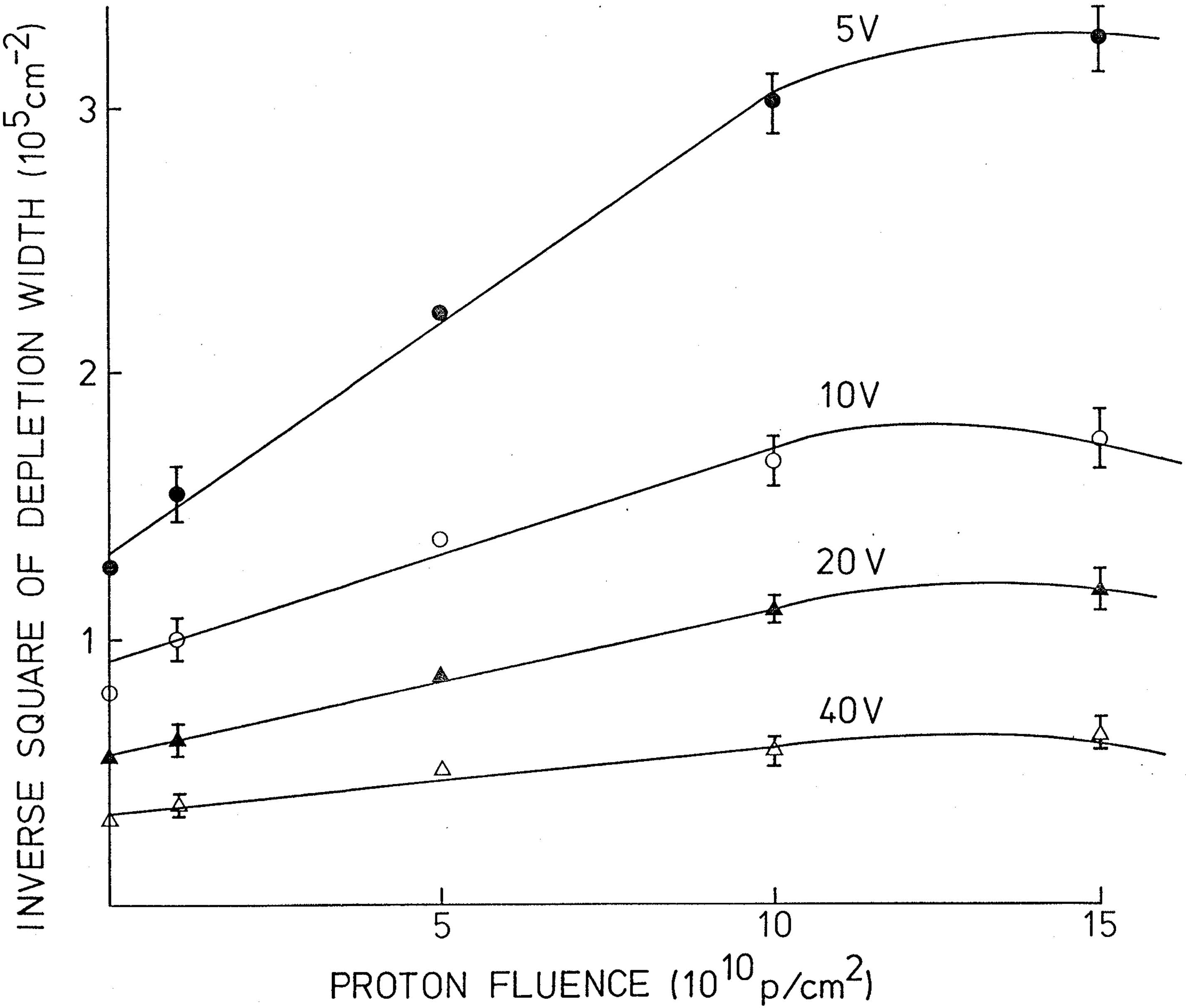

Figure 8. Effect of 40-MeV proton irradiation on the depletion width at several bias voltages.

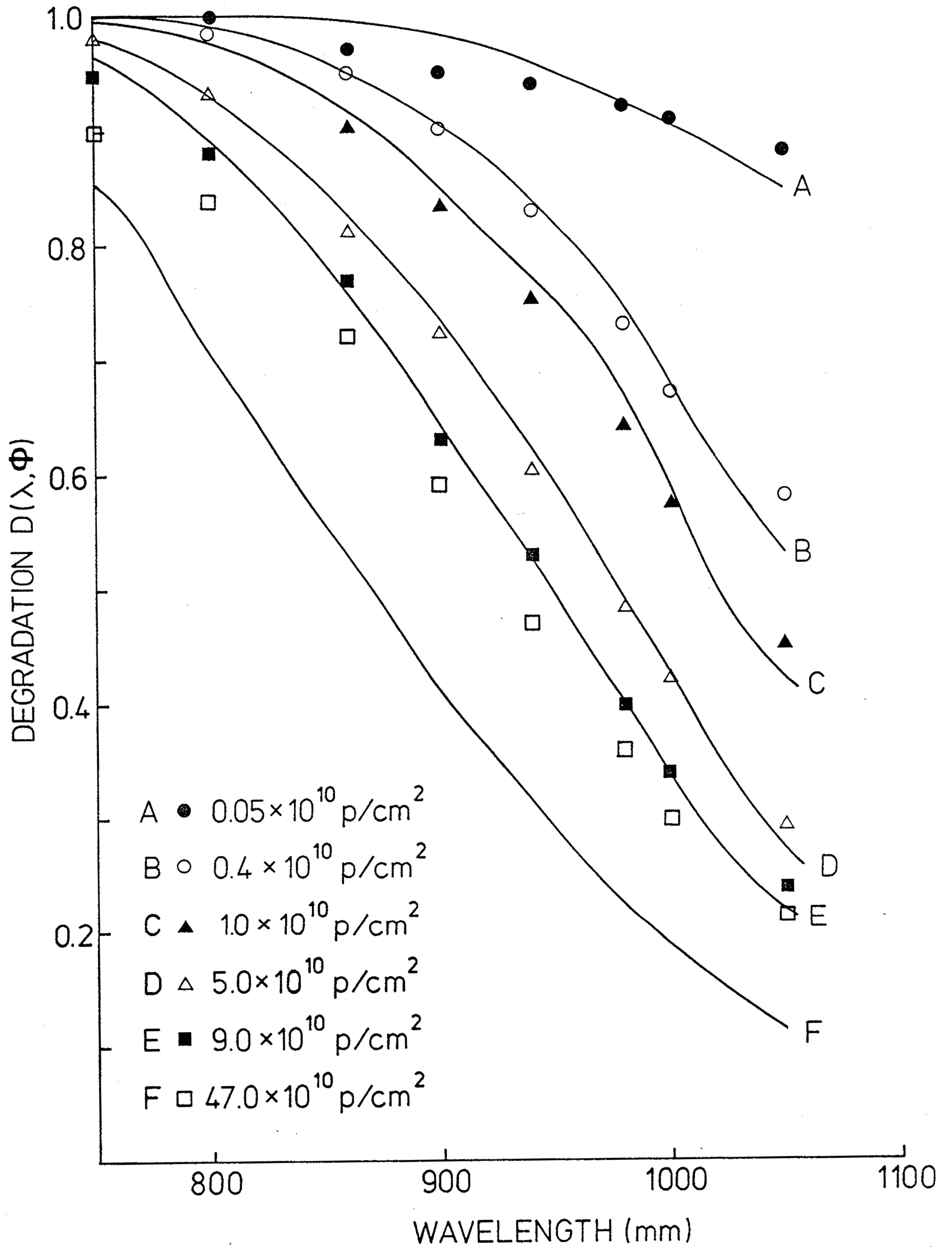

Figure 9. Degradation in spectral response for a typical PIN photodiode irradiated with 40-MeV protons. Symbols indicate experimental data; curves are theoretical fits based on model proposed in text.

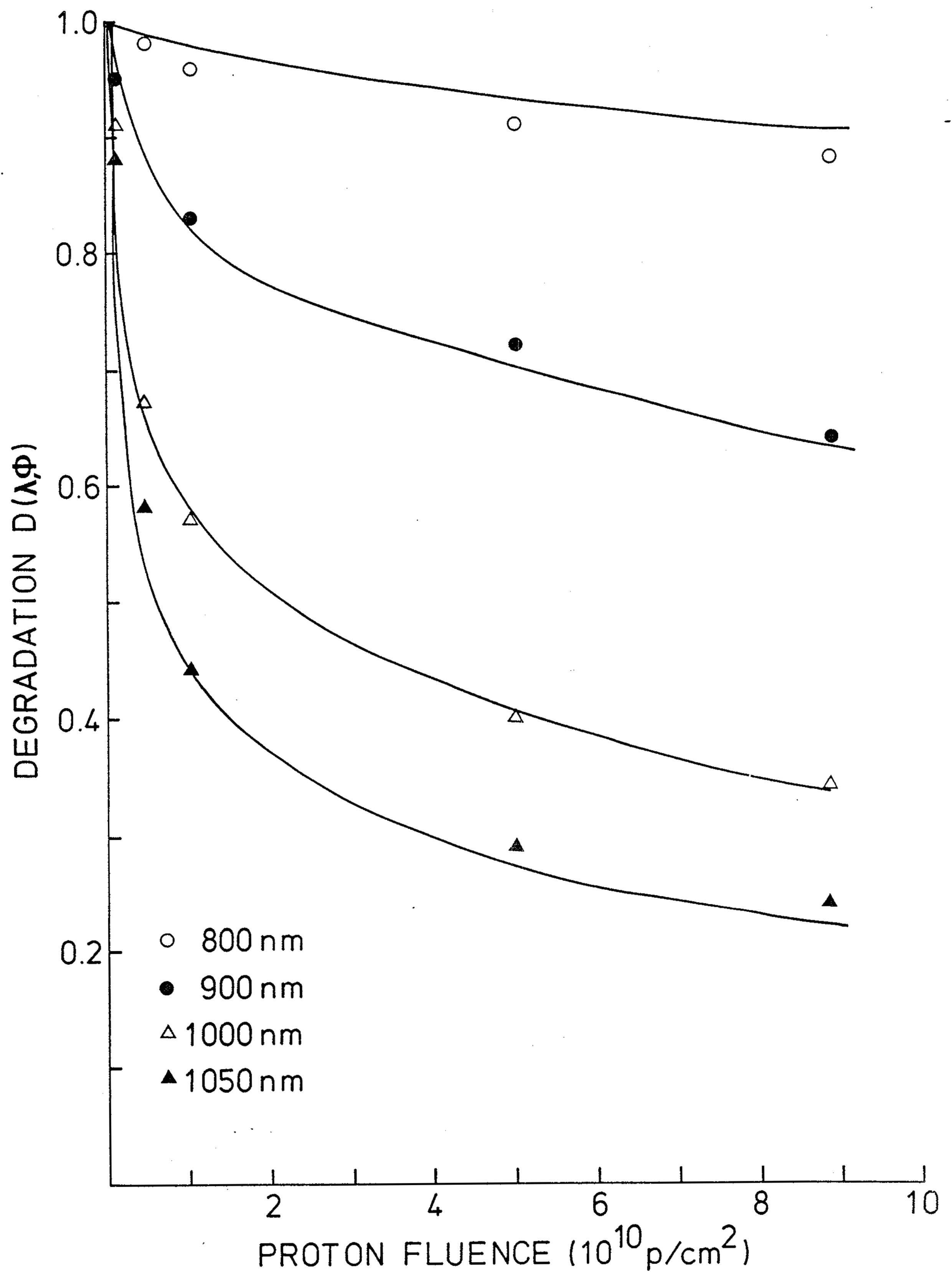

Figure 10. Degradation as a function of fluence at selected wavelengths. Symbols indicate experimental data; curves are theoretical fits based on model proposed in text.

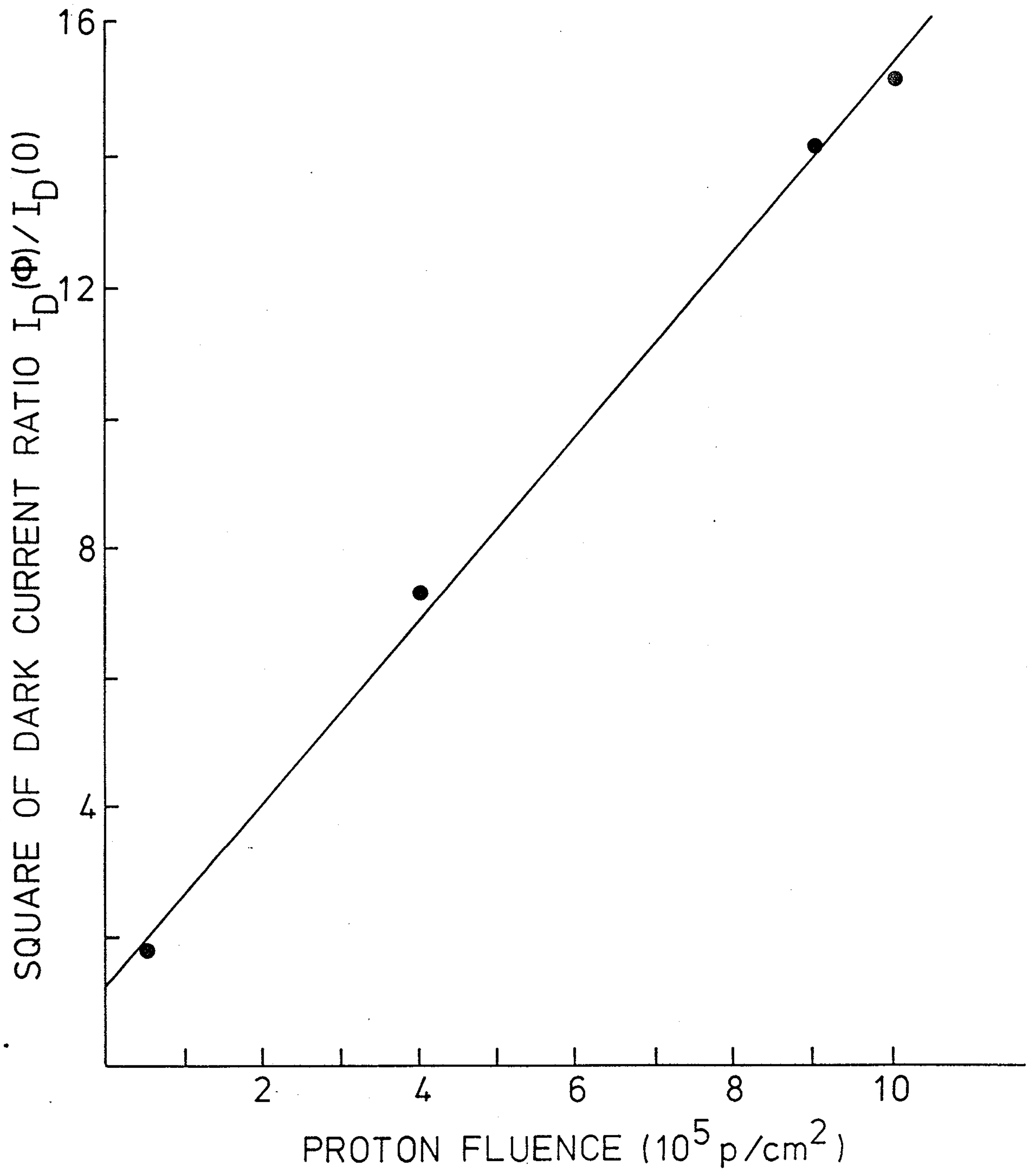

Figure 11. Effect of 40-MeV proton irradiation on PIN photodiode dark current.